Vol. 544: 183–196, 2016
doi: 10.3354/meps11596

MARINE ECOLOGY PROGRESS SERIES
Mar Ecol Prog Ser

Published February 18

When two oceans meet: regional population genetics of an exploited coastal shark, *Mustelus mustelus*

Simo N. Maduna[1,*], Charlene da Silva[2], Sabine P. Wintner[3,4], Rouvay Roodt-Wilding[1], Aletta E. Bester-van der Merwe[1]

[1]Molecular Breeding and Biodiversity Group, Department of Genetics, Stellenbosch University, Private Bag XI, Stellenbosch, 7602, South Africa

[2]Fisheries Research, Department of Agriculture, Forestry and Fisheries, Private Bag X2, Rogge Bay, 8012, South Africa

[3]KwaZulu-Natal Sharks Board, Private Bag 2, Umhlanga Rocks, 4320, South Africa

[4]Biomedical Resource Unit, University of KwaZulu-Natal, Durban, 4000, South Africa

ABSTRACT: The population genetic structure and demographics of the common smoothhound shark *Mustelus mustelus* were investigated across 2 major oceanographic barriers along the southern African coastline: the Angola–Benguela Front and the Indian/Atlantic boundary. Population genetic structure was inferred using multilocus data generated from 8 microsatellite loci and the sequence polymorphism of a 793 bp fragment of the mitochondrial (mtDNA) *ND4* gene region. Microsatellites revealed significant interoceanic genetic structure (F_{ST} = 0.007–0.296) between the South-East Atlantic and South-West Indian Ocean, while mtDNA suggested interoceanic gene flow (pairwise ϕ_{ST} = 0–0.288). A coalescent analysis in MIGRATE-N suggested asymmetrical gene flow that predominantly occurs from the South-West Indian to South-East Atlantic Oceans, with relatively small (<50) estimates of effective population size. Tests of selective neutrality and mismatch distribution indicated a population history consistent with a population expansion event. Contemporary restriction to gene flow is proposed to account for the present-day genetic structuring observed for *M. mustelus* in South Africa. Due to the vulnerable status of the species, these results should be considered in future management and conservation strategies addressing the sustainable exploitation of this fisheries resource.

KEY WORDS: Gene flow · Indian/Atlantic boundary · Interoceanic genetic structure · *Mustelus mustelus* · Oceanographic barrier

INTRODUCTION

Globally, many shark fisheries have been shown to be unsustainable due to the conservative life-history traits (i.e. slow growth rates, late maturity and low reproductive output) of harvested species (Musick et al. 2000, Stevens et al. 2000). Effective management of shark fisheries is further compromised by high rates of misidentification and, hence, a lack of accurate species-specific data (Myers & Worm 2003, Attwood et al. 2011). Genetic data offer valuable information for assessing species composition and are important for characterising genetic variability, defining reproductively isolated stocks and assessing the direction and strength of gene flow between populations (Ovenden 2013). Also, species distributions may extend across national and international boundaries where protection and management legislation may differ for any given species (Ovenden et al. 2013). For any given country, identifying regional

*Corresponding author: simo@sun.ac.za

stocks is, therefore, important for sustainable fisheries management via the allocation of Management Units (MUs). From an evolutionary perspective, it is also important to identify evolutionary significant units (ESUs) (Moritz 1994, Funk et al. 2012).

Delineating finer scale population genetic structure for elasmobranch species has been limited by difficulties of sampling and the general lack of species-specific genetic markers e.g. microsatellites and single nucleotide polymorphisms (SNPs). Cross-species amplification of primer sets from congeneric species is frequently employed as a less costly and time-efficient proxy approach to de novo development of molecular genetic markers (Maduna et al. 2014). When different marker classes are used to delineate population structure, it is important that the results be interpreted with caution to ensure appropriate assignment of MUs and ESUs for short- and long-term conservation, respectively. This is especially important in cases where populations are restricted in distribution, have small population sizes and are subject to human-induced mortality, which is the case for the common smoothhound shark *Mustelus mustelus*.

The common smoothhound shark *M. mustelus* Linnaeus, 1958 is a cosmopolitan species with a widespread distribution from the Mediterranean Sea and eastern Atlantic Ocean to the South-West Indian Ocean. This species is a medium-sized (total length: <1.7 m) epibenthic member of the houndshark family Triakidae (Smale & Compagno 1997). These sharks occur in continental shelf waters of typically <100 m in depth, including intertidal regions, although occurrence at 350 m has been reported in the tropics (Smale & Compagno 1997, Serena et al. 2009). The species is characterised by placental viviparity and a reproductive cycle of 1 yr or longer (Smale & Compagno 1997, Saïdi et al. 2008). *M. mustelus* is harvested commercially and recreationally across the species' range (da Silva & Bürgener 2007). Globally, *M. mustelus* population trends have been recorded as decreasing, and the species is listed as 'Vulnerable' in the IUCN Red List of Threatened Species (da Silva 2007, Serena et al. 2009). Stock assessment of *M. mustelus* in southern Africa by da Silva (2007) indicated that the species is optimally to marginally overexploited, underlining the need for regional conservation and management of this resource. A recent investigation into the movement of smoothhound sharks in Langebaan Lagoon Marine Protected Area (LMPA) found, using telemetry, that this species demonstrated a high degree of site fidelity, with an average distance travelled of 16 km (measured based on the distance between the 2 farthest recorders) (da Silva et al. 2013).

Southern Africa has an extensive and diverse coastline located at the transition zone between the Atlantic and Indo-Pacific biomes (Briggs & Bowen 2012). It offers a unique setting to study the relative importance of oceanography on the genetic structuring of bio-economically important sharks. The South African coastline is characterised by 2 ocean basins [South-East Atlantic Ocean (SEAO) and South-West Indian Ocean (SWIO)] and 3 main temperature-defined bioregions (cool-temperate, warm-temperate and subtropical). Three major current systems circulate around the southern-most point of Africa — the Angola, Benguela and Agulhas currents, which collide to produce the Angola–Benguela and Agulhas–Benguela fronts. These 2 fronts result from the converging of warm, southward-flowing Angola and Agulhas current waters with the cold, northward-flowing Benguela Current (Hutchings et al. 2009, Briggs & Bowen 2012). The impacts of these currents on the population genetic architecture of shark species occurring in this region are poorly understood. Global and regional studies have demonstrated that the Cape Agulhas Boundary, which coincides with the biogeographic disjunction between the cool-temperate Atlantic and warm-temperate Indian biotas (Teske et al. 2011), does not restrict gene flow in cosmopolitan species such as the tope shark (*Galeorhinus galeus*; Chabot & Allen 2009, Chabot 2015) and copper shark (*Carcharhinus brachyurus*; Benavides et al. 2011).

In this study, we assessed patterns of genetic diversity among *M. mustelus* populations along the southern African coast. The alternate hypotheses of panmixia versus population subdivision are tested using multilocus data generated from nuclear-encoded microsatellites and mtDNA *nicotinamide adenine dehydrogenase subunit 4* (*ND4*) sequences. In addition, we investigated the demographic history of *M. mustelus* using the same multilocus data. The number of effective migrants and direction of gene flow among ocean basins were estimated based on microsatellite marker data alone.

MATERIALS AND METHODS

Sample collection and DNA extraction

Seven sampling locations along the South African coast as well as the Dunes, a seascape situated between Tombua and Baia dos Tigres in southern

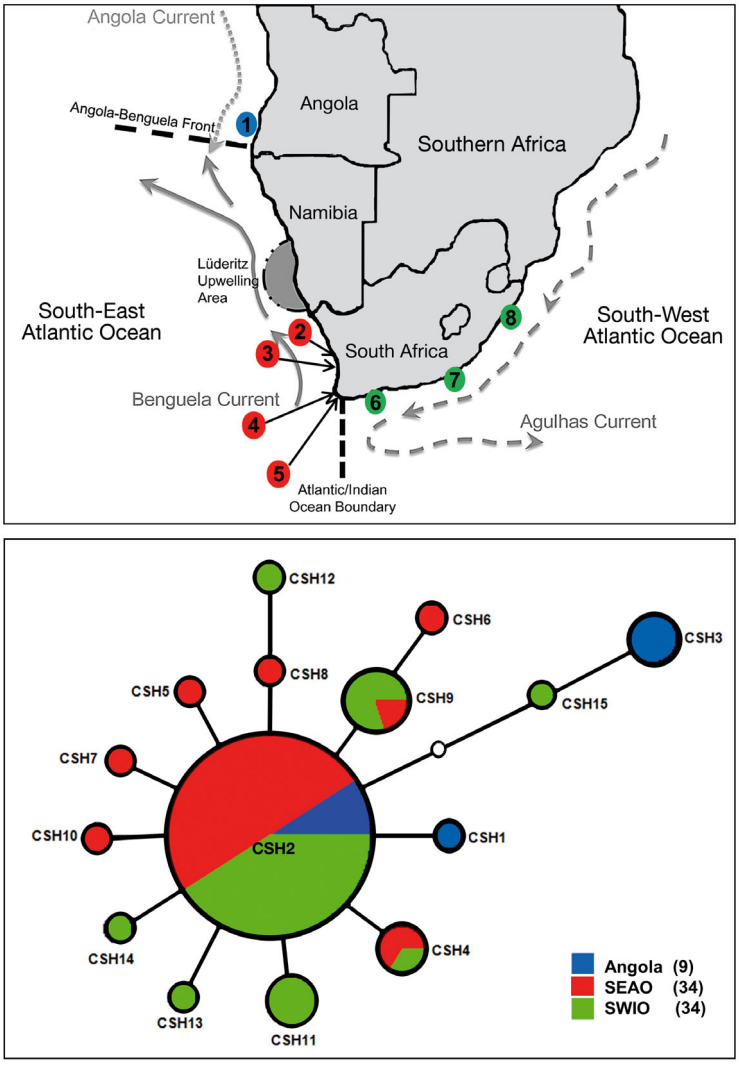

Fig. 1. (a) Sampling localities of *Mustelus mustelus*, with the blue circle representing Angola, and green and red circles representing the South African South-East Atlantic (SEAO) and South-West Indian Ocean (SWIO) sampled populations, respectively. The major oceanographic features are also shown. Angola (ANG, 1), Langebaan Lagoon Marine Protected Area (LMPA, 2), Robben Island (RI, 3), False Bay (FB, 4), Kalk Bay (KB, 5), Struis Bay (SB, 6), Jeffreys Bay (JB, 7) and Durban (DUR, 8). (b) Median-joining network of *M. mustelus* mtDNA *ND4* haplotypes. All haplotypes are separated by 1 mutation, and the white circle represents a hypothetical haplotype not sampled in the study. The sizes of the circles are proportional to the frequency of the haplotypes. See Table 1 for sample numbers

Angola, were included in this study. Tissue samples from a total of 158 houndsharks *Mustelus mustelus* were collected between 2011 and 2013 by licensed shark ecology researchers (see 'Acknowledgements') and one commercial fishing company. Samples comprised either muscle tissue, dorsal- or pelvic-fin clips and were preserved in 95% ethanol. In South African waters, samples were collected from the west (Langebaan Lagoon Marine Protected Area, Robben Island, False Bay and Kalk Bay) and east coasts (Struis Bay, Jeffreys Bay and Durban), representing the 2 main ocean basins (SEAO and SWIO) and Benguela (BC) and Agulhas (AC) Currents, respectively (Fig. 1a). The west coast samples represent SEAO-BC individuals collected west of the proposed Cape Agulhas Boundary, while the east coast samples represent SWIO-AC individuals collected east of the Cape Agulhas Boundary. The samples from southern Angola were located within the Angola Current (ANGC) system in the SEAO, north of a potential hydrodynamic barrier between Angola and South Africa — the Angola-Benguela Front (ABF) (Fig. 1a). Total genomic DNA was isolated using the standard cetyltrimethylammonium bromide (CTAB) method of Saghai-Maroof et al. (1984).

Microsatellite genotyping and mtDNA sequencing

Prior to genotyping, all houndshark samples (158) were screened using the genetic identification method of Farrell et al. (2009) and, in some cases, barcoded using the primers *FishF1* and *FishR1* (Ward et al. 2005). A set of 12 microsatellite markers previously optimised in 2 multiplex reactions — Multiplex Assay 1 (MPS1; *Mh1*, *Mh2*, *Mh9*, *Mh25*, *Mca25* and *McaB39*) and Multiplex Assay 2 (MPS2; *McaB5*, *McaB6*, *McaB22*, *McaB27*, *Mca33* and *McaB37*) — were selected and polymerase chain reaction (PCR) amplification was performed as outlined in Maduna et al. (2014). For subsequent analysis, PCR products were diluted in distilled water, and fragment analysis was performed together with the LIZ600 internal size standard on an ABI 3730XL DNA analyser. Allele scoring was done using GENEMAPPER 4.0 (Life Technologies). Marker efficiency was tested by inspecting genotypic errors resulting from allele dropout, stuttering and null alleles using MICROCHECKER 2.2.3 (Van Oosterhout et al. 2004). Departure from Hardy-Weinberg equilibrium was tested using the exact probability test (500 batches, 10 000 iterations) in

GENEPOP 4.0 (Rousset 2008). Linkage disequilibrium between all pairs of loci was calculated using an exact test also implemented in GENEPOP. The F_{ST}-outlier method as implemented in LOSITAN 1.44 (10 000 permutations assuming the infinite alleles model) was used to test for neutrality (Antao et al. 2008).

For mtDNA analysis, a subset of 78 individuals from across the 8 sampling locations was included to investigate the congruence between microsatellites and mtDNA patterns of genetic diversity and differentiation. The mitochondrial gene *ND4* was targeted and amplified for each individual using the primers *MaND4F* and *MaND4R* according to Boomer et al. (2010). The PCR amplicons were bi-directionally sequenced using the standard Sanger sequencing chemistry (BigDye® terminator v3.1 cycle sequencing kit; Life Technologies) at Stellenbosch University Central Analytical Facility. Sequences were aligned in MEGA v5.2 (Tamura et al. 2011), manually corrected and trimmed to equal lengths, and unique haplotypes were subsequently identified in ARLEQUIN 3.5 (Excoffier & Lischer 2010). Maximum-parsimony haplotype networks were constructed using the median joining algorithm (Bandelt et al. 1999) with default parameters in the software NETWORK 4.6.1.2 (www.fluxus-engineering.com).

Population analysis

Genetic diversity was measured as the number of alleles (A_N) per locus, observed heterozygosity (H_O) and expected heterozygosity (H_E) was calculated using GENALEX 6.5 (Peakall & Smouse 2012), polymorphic information content (PIC) was calculated in MSATTOOLS 1.0 (Park 2001) and allelic richness was standardized for sample sizes (A_R) calculated in HP-RARE 1.0 (Kalinowski 2005). The following mtDNA *ND4* sequence diversity parameters were estimated for each sampling population using DNASP 5.10 (Librado & Rozas 2009): number of polymorphic sites (S), number of haplotypes (N_H), haplotype diversity (h) and nucleotide diversity (π). Pairwise F_{ST} (Weir & Cockerham 1984) and Jost's D_{est} (Jost 2008) estimates between sampling populations were calculated in GENALEX. A hierarchical locus by locus analysis of molecular variance (AMOVA), with 1000 permutations to determine significance, was computed in ARLEQUIN; groups were based on oceanic current system origin (ANGC, BC, or AC system) to test the *a priori* hydrodynamic barrier between Angola and South Africa — the ABF. Additionally, hierarchical AMOVA was used to examine the *a priori* biogeographic barrier across the SEAO (including Angola) and SWIO — the Cape Agulhas Boundary. Isolation by distance (IBD) was tested using a Mantel test in GENALEX. The Bayesian clustering model-based method implemented in STRUCTURE 2.3 (Pritchard et al. 2000) was used to detect the most likely number of genetic clusters (K) present in the southern African samples. The admixture model with correlated allele frequencies was applied for 10 replicates across K = 1 (panmixia) to K = 8 (each sampling site distinct), with each run consisting of 2 000 000 Markov chain Monte Carlo (MCMC) iterations and an initial burn-in phase of 200 000 iterations assuming no prior population information. The program STRUCTURE HARVESTER 0.3 (Earl & vonHoldt 2012) was used to infer the ΔK statistic suggested by Evanno et al. (2005). Subsequent runs (200 000 burn-in and 2 000 000 MCMC iterations) were executed to detect the presence of sub-structure within each cluster when $K > 1$ was identified at the oceanic scale. The results from the 10 replicates were averaged using the software CLUMPP 1.1 (Jakobsson & Rosenberg 2007), and the output was visualised using DISTRUCT 1.1 (Rosenberg 2004).

For the *ND4* sequence data, the degree of genetic differentiation among populations was estimated using pairwise Φ_{ST} values (with significance determined using 1000 bootstrapped replicates) computed in ARLEQUIN. No corrections for multiple tests were made, as significance values were present for all pairwise comparisons. Hierarchical population structure was evaluated through AMOVA testing the same grouping hypotheses as for the microsatellites. The best available model in ARLEQUIN for these analyses was the Tamura-Nei model as determined by the maximum-likelihood test implemented in JMODELTEST 2.0 (Darriba et al. 2012), with models ranked using Akaike and Bayesian information criterion (AIC and BIC, respectively) with correction for small sample size.

Demographic and gene flow analysis

The occurrence of recent bottlenecks and changes in effective population size were evaluated using the Wilcoxon signed-rank test for significant deviation from heterozygosity excess and deficiency under all 3 mutation models [infinite alleles model (IAM), stepwise mutation model (SMM) and the 2-phased model (TPM)] implemented in the program BOTTLENECK

1.2 (Piry et al. 1999). Analysis in BOTTLENECK was performed using 1000 replications at the 5% nominal level under the 3 different models. For the TPM, the proportions were in favour of the SMM (90% SMM and 10% IAM), with a variance of 30. Furthermore, the qualitative test of model shift was performed to calculate the allele frequency distribution using BOTTLENECK.

Demographic analyses using the mtDNA sequence data were performed in ARLEQUIN. Harpending's raggedness index (H_{RI}; Harpending 1994) was estimated for each sampling populations (20 000 permutations) to infer changes in population size based on the frequency of pairwise differences among haplotypes (Schneider & Excoffier 1999). Deviations from selective neutrality were also tested with Tajima's D (Tajima 1989) and Fu's F_s (Fu 1997) (20 000 permutations; $\alpha = 0.05$ and $\alpha = 0.02$, respectively) based on an infinite-site model without recombination. Furthermore, selective neutrality was tested in DNASP using the Fu & Li's F^* & D^* statistics (Fu & Li 1993) to differentiate between demographic processes such as a population expansion and genetic hitchhiking or background selection. Divergence from an ancestral population size Θ_0 at T-generations in the past was estimated over all sampling sites. The value of T, scaled by the mutation rate μ, i.e. $\tau = 2\mu T$, was estimated assuming (1) isolation after divergence and (2) constant but unequal populations sizes (Schneider & Excoffier 1999).

To gain an understanding of the impacts of southern African oceanic currents on the population genetic structure of *Mustelus mustelus*, the coalescence-based method was used to compare alternative migration patterns between oceans. This method was performed in the program MIGRATE-N 3.6.11 (Beerli 2006, Beerli & Palczewski 2010) implemented on the CIPRES Portal v3.3 at the San Diego Supercomputer Center (Miller et al. 2010). The populations were grouped according to ocean basin origin [SEAO (including Angola) and SWIO]. Four migration models were evaluated: (1) a full model with 2 population sizes and 2 migration rates (from SEAO to SWIO and from SWIO to SEAO), (2) a model with 2 population sizes and 1 migration rate to SEAO; (3) a model with 2 population sizes and 1 migration rate to SWIO and (4) a model where SEAO and SWIO are part of the same panmictic population.

MIGRATE-N also estimated the mutation-scaled effective population size $\Theta = 4N_e\mu$, where N_e is the effective population size and μ is the mutation rate per generation per locus, as well as the mutation-scaled migration rates $M = m/\mu$, where m is the immigration rate per generation among populations. A Brownian process was used to model microsatellite mutation. The Metropolis-Hastings algorithm was used to sample from the prior distributions and generate posterior distributions. Each model was run using random genealogy, and values of the parameters Θ and M were generated by F_{ST} calculation as the starting condition. Bayesian search strategy was conducted using the following parameters: an MCMC search of 5×10^5 burn-in steps, followed by 5×10^6 steps with parameters recorded every 20 steps. The prior distribution for the parameters was uniform, with boundaries defined after explorative runs, Θ (min.: 0.0, max.: 10.0, delta: 1.0) and migration (min.: 0.0, max.: 50.0, delta: 5.0). A static heating scheme with 4 different temperatures (1.0, 1.5, 3.0, 1×10^6) was employed, where acceptance–rejection swaps were proposed at every step. The model comparison was done using log-equivalent Bayes factors (LBF) that need the accurate calculation of marginal likelihoods. These likelihoods were calculated using thermodynamic integration in MIGRATE-N. Models were ordered by LBF, and the model probability (p_{Mi}) was calculated in R (R Development Core Team 2013) by following the procedure described in the MIGRATE-N Tutorial (http://molevol.mbl.edu/wiki/index.php/Migrate_tutorial).

RESULTS

To ensure correct species identification prior to population genetic analysis, all 158 houndshark samples were screened and 144 (91.1%) were positively identified as *Mustelus mustelus*. The remaining samples were identified as other triakid species, such as *Galeorhinus galeus* and *M. palumbes*, based on the combination of *COI* barcoding and the identification method of Farrell et al. (2009). Misidentified individuals were excluded from further analyses.

Genetic diversity

Microsatellites

A total of 113 alleles were observed across all loci, with allele numbers ranging from 2 to 14 per locus. No genotyping errors, due to stuttering or allelic dropout, were identified. Fixation indices (F_{IS}) were highly significant in most sampling populations, with values ranging from −1 to 0.835, mostly due to significant heterozygote excess or deficiencies at some

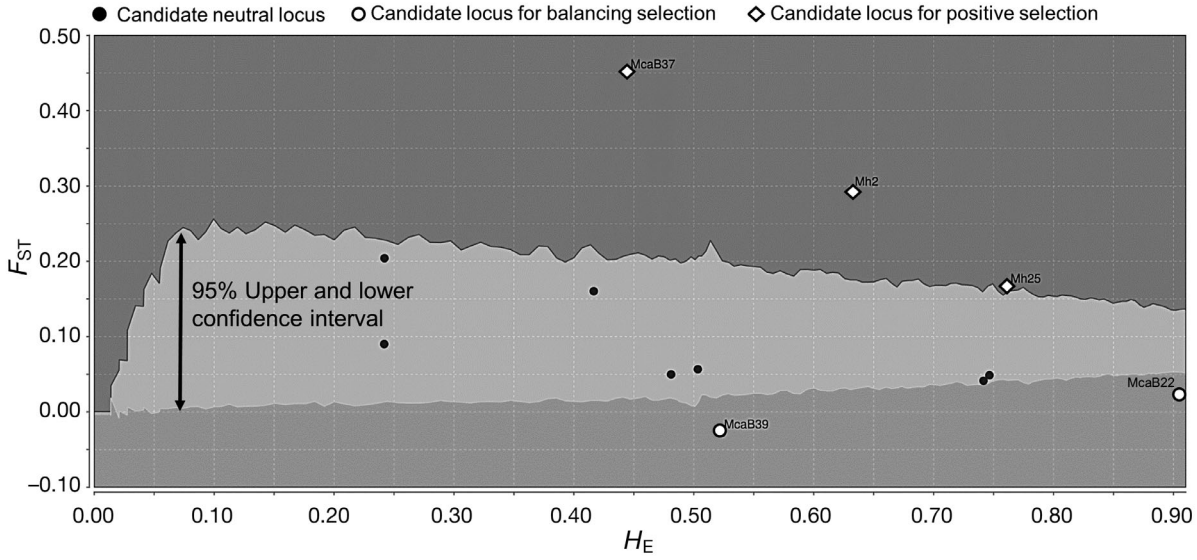

Fig. 2. LOSITAN results indicating outlier loci as candidate loci under directional (white squares in upper area) and balancing selection (white circles in lower area)

loci (see Table S1 in the Supplement at www.int-res.com/articles/suppl/m544p183_supp.pdf). Null alleles were present at some loci (*Mh2* and *Mh25*) at significantly high frequencies ($p < 0.05$) and most likely explain the observed deviations from Hardy-Weinberg expectation at these loci (Table S1). The F_{ST}-outlier test showed that 5 loci did not conform to neutrality (*McaB22* and *McaB39* [under balancing selection]; *McaB37*, *Mh2* and *Mh25* [under directional selection]) (Fig. 2). Genetic diversity, based on all measures, varied from low to moderate (mean: $4 \leq A_N \leq 9$; mean: $0.400 \leq H_E \leq 0.600$) across the sampling populations (Table 1). Three of the 66 pairs of loci were in linkage disequilibrium ($p < 0.01$): *Mh9–Mca25*, *McaB5–McaB6* and *McaB27–Mca33*. Subsequent estimates of population genetic structure and analyses of demographic history were therefore computed using a subset of 8 microsatellites, excluding loci not conforming to Hardy-Weinberg equilibrium, neutrality, and/or exhibiting high null allele frequencies (*Mh2*, *Mh25*, *McaB22* and *McaB39*).

mtDNA

A 793 bp fragment of the mitochondrial *ND4* locus was successfully amplified and sequenced for 78 *M. mustelus* samples. A total of 15 polymorphic sites (*S*), of which 7 were parsimony informative and 8 were

Table 1. Genetic variation descriptors at 12 microsatellite loci and a 793 bp fragment of the mitochondrial DNA *ND4* region in *Mustelus mustelus* in southern Africa, including the number of individuals (n), mean number of alleles per locus (A_N/locus), allelic richness (A_R), observed heterozygosity (H_O), expected heterozygosity (H_E), polymorphic information content (PIC), within-location inbreeding coefficient (F_{IS}), number of haplotypes (N_H, unique haplotypes in parentheses), haplotype diversity (h) and nucleotide diversity (π). See Fig. 1 for location abbreviations

Population	Nuclear microsatellites							Mitochondrial *ND4* sequences			
	n	A_N/locus	A_R	H_O	H_E	PIC	F_{IS}	n	N_H	h	π
ANG	12	4.0	2.1	0.453	0.504	0.433	0.041	9	3 (2)	0.639	0.0022
LMPA	24	3.9	1.9	0.410	0.427	0.377	0.011	13	2 (0)	0.154	0.0002
RI	22	4.2	2.0	0.404	0.439	0.395	0.103	8	4 (3)	0.643	0.0013
FB	17	5.1	2.1	0.490	0.504	0.448	0.040	6	3 (1)	0.600	0.0008
KB	16	2.2	2.2	0.558	0.528	0.46	–0.063	7	2 (1)	0.286	0.0004
SB	17	3.8	2.1	0.654	0.527	0.449	–0.234	12	2 (1)	0.409	0.0005
JB	16	5.2	2.3	0.583	0.597	0.531	–0.012	10	2 (0)	0.200	0.0003
DUR	20	4.6	2.2	0.467	0.526	0.468	0.078	13	7 (4)	0.846	0.0019

Table 2. Pairwise genetic distances between sampling locations for *Mustelus mustelus* based on microsatellite variation and the *ND4* region. F_{ST} and Φ_{ST} values are below and above the diagonal, respectively. Significance from 10000 permutations of the data matrix (p-value) is shown in parentheses for each fixation index; p-values < 0.05 are shown in **bold**. See Fig. 1 for location abbreviations

	ANG	LMPA	RI	FB	KB	SB	JB	DUR
ANG		0.246 (0.052)	0.230 (**0.047**)	0.171 (0.142)	0.174 (0.172)	0.288 (**0.015**)	0.206 (0.087)	0.158 (**0.028**)
LMPA	0.072 (**0.001**)		0.008 (0.531)	0.052 (0.223)	0.028 (0.328)	0.159 (0.055)	−0.093 (0.999)	−0.045 (0.865)
RI	0.090 (**0.001**)	0.007 (0.191)		−0.087 (0.887)	−0.027 (0.797)	0.154 (**0.048**)	−0.012 (0.582)	−0.056 (0.863)
FB	0.053 (**0.003**)	0.033 (**0.005**)	0.043 (**0.003**)		0.020 (0.370)	0.087 (0.086)	0.025 (0.315)	−0.123 (0.982)
KB	0.103 (**0.001**)	0.150 (**0.001**)	0.172 (**0.001**)	0.039 (**0.007**)		0.103 (0.137)	0.013 (0.386)	−0.038 (0.765)
SB	0.200 (**0.001**)	0.207 (**0.001**)	0.175 (**0.001**)	0.201 (**0.001**)	0.296 (**0.001**)		0.136 (0.161)	−0.061 (0.909)
JB	0.078 (**0.001**)	0.110 (**0.001**)	0.088 (**0.001**)	0.045 (**0.002**)	0.075 (**0.001**)	0.134 (**0.001**)		0.013 (0.271)
DUR	0.180 (**0.001**)	0.171 (**0.001**)	0.145 (**0.001**)	0.129 (**0.001**)	0.210 (**0.001**)	0.132 (**0.001**)	0.082 (**0.001**)	

singletons, characterised 15 haplotypes (Table 1; Table S2 in the Supplement). The haplotype network incorporating the 8 putative populations showed a distinct starlike pattern, characterised by one central haplotype (CSH2) surrounded by an array of low-frequency variants (CSH1; CSH3–CSH15) (Fig. 1b). A high degree of haplotype sharing was observed among the sampling areas, with the central haplotype (CSH2, n = 54) present at all locations. Two lower frequency haplotypes (CSH4 and CSH9) were also shared amongst 2 or more locations. The haplotype network revealed 2 unique haplotypes among the Angolan samples — CSH1 and CSH3, the latter of which being shared by 3 individuals. This provides some evidence suggestive of a restriction in gene flow of this population from those in South African waters. For pooled sample locations, overall haplotype (h) and nucleotide diversity (π) were 0.517 ± 0.069 and 0.00104 ± 0.00386, respectively (Table 1). The patterns of genetic diversity did not show any consistence with geographical features, and across sampling locations genetic diversity ranged from low to high, being highest at Durban (h = 0.846, π = 0.00194) and lowest at Langebaan (h = 0.154, π = 0.00019).

Population differentiation

Microsatellites

Pairwise F_{ST} estimates, ranging from 0.007 to 0.296, were congruent with the results obtained for Jost's D_{est} (Table S3 in the Supplement), and most of the estimates were statistically significant amongst the putative populations ($p < 0.05$; Table 2). Notably, F_{ST} estimates were large (i.e. ≥0.120) for almost all Atlantic versus Indian Ocean comparisons; this corroborates the 2 distinct oceanic clusters obtained with the STRUCTURE results (Fig. 3). Hierarchical AMOVA for the 3 oceanic current region groups (ANGC vs. SEAO-BC vs. SWIO-AC) supported regional population genetic structure at all levels, with significant differentiation amongst regions (F_{CT} = 0.084, $p < 0.01$), within regions (F_{SC} = 0.055, $p < 0.01$) and over all regions and populations (F_{ST} = 0.134, $p < 0.01$) (Table 3). Hierarchical AMOVA for the oceanic clusters (Angola+SEAO populations vs. SWIO populations) also indicated the restriction of gene flow of the oceans, with significant differentiation amongst oceans (F_{CT} = 0.097, $p < 0.01$), within oceans (F_{SC} = 0.071, $p < 0.01$) and within populations (F_{ST} = 0.161,

Table 3. Hierarchical AMOVA results for different grouping hypotheses of *Mustelus mustelus* based on ocean basins or proposed barriers; $^{*}p < 0.05$, $^{**}p < 0.01$

Population grouping	Source of variation	Microsatellites			*ND4*		
		Variation (%)	*F*-statistic	p-value	Variation (%)	Φ-statistic	p-value
Angola vs. Benguela vs. Agulhas Current populations	Among regions	8	F_{CT} = 0.084	0.001**	15	Φ_{CT} = 0.151	0.043*
	Within regions	5	F_{SC} = 0.055	0.000**	−2	Φ_{SC} = −0.027	0.538
	Within populations	87	F_{ST} = 0.134	0.000**	87	Φ_{ST} = 0.128	0.007**
Angola + Atlantic Ocean populations (SEAO) vs. Indian Ocean populations (SWIO)	Among oceans	10	F_{CT} = 0.097	0.000**	−0.33	Φ_{CT} = −0.003	0.521
	Within oceans	6	F_{SC} = 0.071	0.003**	8.72	Φ_{SC} = 0.087	0.002**
	Within populations	84	F_{ST} = 0.161	0.000**	91.62	Φ_{ST} = 0.084	0.005**

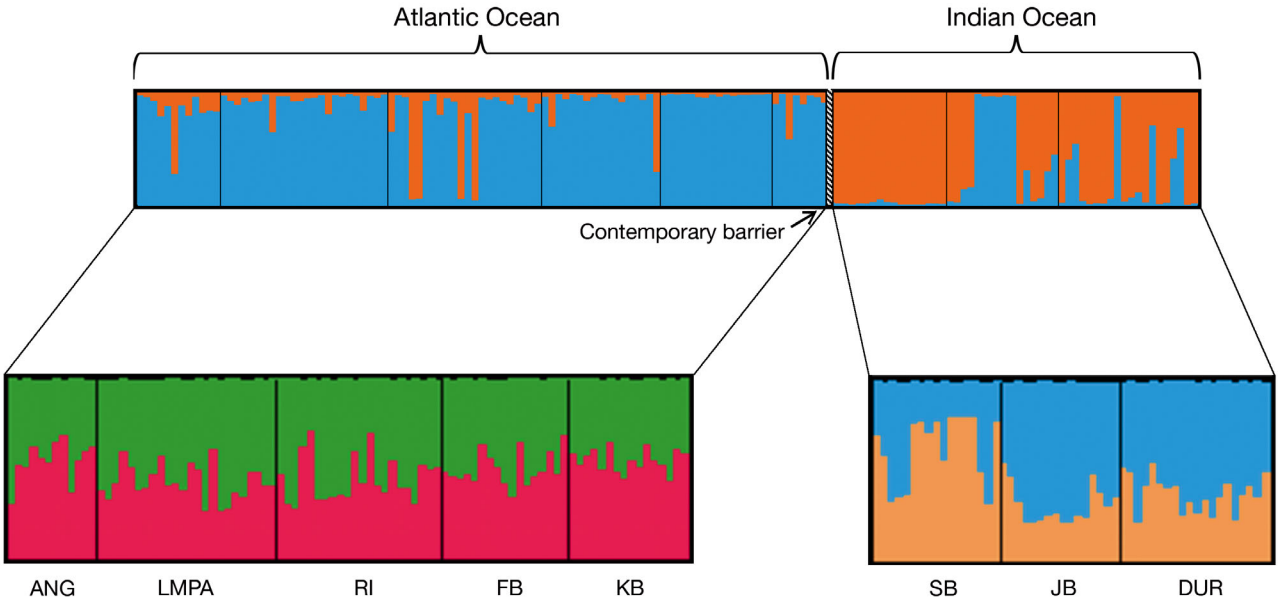

Fig. 3. STRUCTURE results showing a hierarchical genetic structure of *Mustelus mustelus* populations. Bar plots showing individual genotype membership to *K* clusters (each cluster is represented by a different colour, and each vertical bar represents an individual). STRUCTURE was initially run with all samples in southern Africa ($K = 2$ shown), followed by subsequent runs for South-East Atlantic Ocean ($K = 2$ shown) and South-West Indian Ocean ($K = 2$ shown) individually. See Fig. 1 for abbreviations

$p < 0.01$) (Table 3). When considering the entire dataset, there was no significant correlation between genetic and geographic distances (isolation by distance; IBD) at microsatellite loci ($r^2 = 0.0025$, $p = 0.584$; Fig. S1a in the Supplement). Similarly, excluding the peripheral population of Angola, the data did not support significant IBD, possibly due to sampling noise associated with our F_{ST} estimates ($r^2 = 0.1152$, $p = 0.162$; Fig. S1c). Bayesian clustering analysis in STRUCTURE also supported population subdivision in the study area. More specifically, it proposed the clustering of the SWIO populations separate from the rest, hence identifying the most likely number of populations as $K = 2$ based on the Evanno et al. (2005) method (ΔK statistic; Fig. 3 and Fig. S2 in the Supplement). Subsequent STRUCTURE runs on each of these genetic clusters revealed sub-structure within oceans.

mtDNA

Genetic differentiation based on population pairwise Φ_{ST} estimates varied, ranging from 0 to 0.288 (Table 2), and were non-significant for almost all population comparisons. Exceptions to this include significant Φ_{ST}-values between Angola and 3 of the South African populations (Robben Island, Struis Bay and Durban), and between Robben Island and Struis Bay. The AMOVA analysis detected genetic subdivision between the Angolan, SEAO and SWIO populations, with significant differentiation amongst regions ($\Phi_{CT} = 0.151$, $p = 0.043$) and within putative populations ($\Phi_{ST} = 0.128$, $p = 0.007$) (Table 3). However, there was a lack of within-region genetic variation ($\Phi_{SC} = -0.027$, $p = 0.538$), suggestive of insufficient time that has passed to detect stronger within-region differentiation between putative populations with this particular marker. In addition, no genetic structure was detected between the SEAO (including Angola) and SWIO oceanic regions (Table 3). The haplotype network revealed no relationship between haplotype genealogy and geographic location, but supported the existence of past and/or contemporary genetic connectivity between populations (Fig. 1b)—for instance, haplotypes CSH2, CSH4 and CSH9 were shared by both Atlantic and Indian Ocean populations. Mantel tests revealed a positive and significant correlation between Φ_{ST} and geographic distance, indicating a pattern of IBD when all populations were compared ($r^2 = 0.642$, $p = 0.017$; Fig. S1b). However, when considering only populations along the South African coastline, no correlation between Φ_{ST} and geographic distance was detected ($r^2 = 0.0405$, $p = 0.185$; Fig. S1d).

Table 4. Signed rank Wilcoxon test of the mutation–drift equilibrium estimated for 8 microsatellite loci at 8 *Mustelus mustelus* sampling sites in southern Africa. Significant values ($p < 0.05$) of the 1-tailed test for H_E excess ($p_{HE\text{-}excess}$) and deficiency ($p_{HE\text{-}deficiency}$) under the infinite alleles model (IAM), a stepwise mutation model (SMM) and the 2-phase model (TPM) are highlighted in **bold**. See Fig. 1 for location abbreviations

Population	Mutation model					
	IAM		SMM		TPM	
	$p_{HE\text{-}deficiency}$	$p_{HE\text{-}excess}$	$p_{HE\text{-}deficiency}$	$p_{HE\text{-}excess}$	$p_{HE\text{-}deficiency}$	$p_{HE\text{-}excess}$
ANG	0.656	0.422	**0.039**	0.977	0.055	0.961
LMPA	0.148	0.945	**0.012**	0.992	**0.027**	0.980
RI	0.406	0.656	**0.027**	0.980	0.055	0.961
FB	0.191	0.844	**0.006**	0.996	**0.014**	0.990
KB	0.422	0.629	**0.004**	0.998	**0.020**	0.986
SB	0.945	0.148	0.766	0.289	0.945	0.148
JB	0.422	0.629	**0.010**	0.994	**0.020**	0.986
DUR	0.406	0.656	**0.020**	0.988	**0.020**	0.988

Demographic history and gene flow

Microsatellites

There was no significant heterozygosity excess identified in any putative population under any of the 3 mutation models (TPM, SMM, or IAM; Wilcoxon signed-rank test, $p > 0.05$). These results were consistent with the normal L-shaped distribution of allele frequency (Fig. S3 in the Supplement), indicating no genetic bottleneck in any of the 8 sample populations in the recent past. Rather, significant heterozygosity deficiency observed across all the sampling populations (but excluding Struis Bay) under the SMM provided evidence of a recent demographic expansion event (Wilcoxon signed-rank test: SMM, $p < 0.05$; Table 4). Under the TPM, all the sampling populations, but excluding Angola, Robben Island and Struis Bay, displayed significant heterozygosity deficiency.

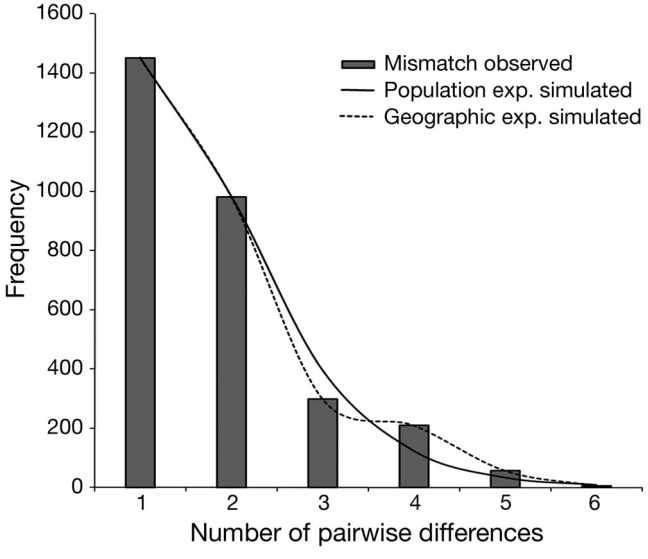

Fig. 4. Mismatch distribution among *ND4* sequences of *Mustelus mustelus* in southern Africa: the observed distribution (grey columns) versus the simulated distribution under a population expansion model (solid line) and a geographic expansion model (broken line)

mtDNA

Overall, Tajima's *D* and Fu's *F* statistics for neutrality were negative and non-significant ($D = -0.783$, $p > 0.05$ and Fs $= -0.505$, $p > 0.05$, respectively), indicating no excess of alleles that would be expected following a population expansion event (Fu 1997). Fu & Li's F^* and D^* were significant ($F^* = -2.820$, $p < 0.05$; $D^* = -2.529$, $p < 0.05$), indicating a deficiency of recent mutations due to background selection. Mismatch distributions, however, were consistent with the sudden population expansion model (Fig. 4), which could not be rejected by any of the tests performed — sum of square distances (SSD; $p_{(Sim.\ SSD \geq Obs.\ SSD)} = 0.677$) and Harpending's raggedness index ($p_{(Sim.\ Rag. \geq Obs.\ Rag.)} = 0.805$). Taking into account all the sample sites, the mismatch analysis estimated an ancestral population size (Θ_0) of 0.3 and an actual population size (Θ_1) of 5.1, with a τ-value of 0.5. The large difference between Θ_0 and Θ_1 resulted in a large Θ-ratio ($\Theta_1/\Theta_0 = 17$), which is indicative of population expansion.

Coalescent analyses for migration model comparison highly supported ($p = 1.0$) Model 2 (i.e. migration from SWIO to SEAO) and showed that Θ was highest in the SWIO-AC ($\Theta = 6.070$) and lowest in the SEAO-BC ($\Theta = 1.190$). Model 2 states that there is unidirectional gene flow from east to west ($M_{SWIO \rightarrow SEAO} = 19.850$, $N_{m\ SWIO \rightarrow SEAO} = 9.253$) (Table 5).

DISCUSSION

Genetic structure

In southern Africa, the common smoothhound sharks *Mustelus mustelus* have a wide and continuous distribution. Interestingly, existing tag data for the common smoothhound shark are limited, but have indicated that the species has a high degree of site fidelity (da Silva et al. 2013). Here we found evi-

Table 5. Log Bayes factor (LBF) using thermodynamic integration of different gene flow models M_i compared with Model 2 for 2 sampling ocean basins of *Mustelus mustelus* (A: South-East Atlantic Ocean; I: South-West Indian Ocean); p_{Mi} is the model choice probability. lmL: log marginal likelihood

Model	Parameters [97.5% CI]	Bézier lmL	LBF for model	Rank of model	p_{Mi}
1 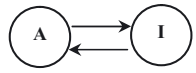	Θ_A = 2.110 [1.300–3.080] Θ_I = 4.670 [3.040–6.400] $M_{I\rightarrow A}$ = 5.450 [2.800–10.500] $M_{A\rightarrow I}$ = 3.250 [1.700–4.100]	−29938.51	−3832.30	3rd	0
2 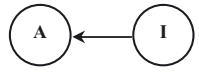	Θ_A = 1.190 [0.460–1.700] Θ_I = 6.070 [4.780–7.220] $M_{I\rightarrow A}$ = 19.850 [9.100–35.100]	−28022.36	0.00	1st	1
3 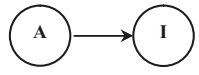	Θ_A = 4.710 [3.700–5.600] Θ_I = 4.230 [2.020–7.500] $M_{A\rightarrow I}$ = 8.750 [5.600–14.800]	−28056.60	−68.48	2nd	1.35×10^{-15}
4 	$\Theta_{A,I}$ = 6.190 [5.020–7.360]	−40130.44	−24216.00	4th	0

dence of fine-scale population genetic structure of the species across this region. We rejected the null hypothesis of panmixia in *M. mustelus* in southern African waters based on the nuclear microsatellite data and to a limited extent by mtDNA *ND4* sequence data. The microsatellite data detected the existence of 2 management units (SEAO and SWIO), while the mtDNA implied the possible existence of 2 evolutionary significant units (Angola and South Africa) across the sampling area. More specifically, the microsatellite data suggest intraoceanic and interoceanic population structure for *M. mustelus* in southern Africa. This signal of contemporary genetic clustering is most likely a consequence of sampling of populations along a gradient of restricted gene flow, hence hierarchical genetic structure and possible spatial autocorrelation. Similar population structuring has been demonstrated for a range of related, but less mobile, sharks species in other regions of the world where intraspecific populations are connected via a series of stepping stone populations, e.g. the narrownose smoothhound *Mustelus schmitti* (Pereyra et al. 2010), the Australian gummy shark *M. antarticus* (Boomer 2013), the rig *M. lenticulatus* (Boomer 2013) and the brown smoothhound shark *M. henlei* (Chabot et al. 2015). Chabot et al. (2015) investigated population connectivity of the brown smoothhound shark across prominent biogeographic and phylogeographic barriers of the northeastern Pacific and found restricted gene flow between the northern and central populations.

Mitochondrial *ND4* sequence data on the other hand indicated that, historically, *M. mustelus* populations in South Africa (excluding Angola) constituted a single population, with high levels of interoceanic gene flow across the Cape Agulhas Boundary for this species. This is consistent with the hypothesis that the leakage of the Agulhas Current during the warm interglacial periods throughout the Pleistocene epoch enabled gene flow between Atlantic and Indian Ocean populations (Peeters et al. 2004), suggesting that not enough time has passed to fix any subsequent population-specific mutations at the mtDNA level. The *ND4* sequence data did however reveal significant genetic divergence between the Angolan and 3 South African populations (Robben Island, Struis Bay and Durban). In doing so, this study presents evidence of the Angola–Benguela Front being a semi-permeable barrier to gene flow between South Africa and Angola.

The directionality of gene flow (i.e. the number of migrants per generation) was southwards between the oceanic regions tested, indicating the likely effects of ocean currents and temperature gradients on the degree and directionality of gene flow. The Benguela Current and its interplay with the Agulhas Current are often cited as important barriers to dispersal of southern African coastal fishes (Henriques et al. 2012, 2014, 2015). Our results indicated that interoceanic gene flow for *M. mustelus* was restricted at the Cape Agulhas Boundary, suggesting that the Agulhas Current plays a prominent role in limiting

dispersal in an eastward direction. For a few other actively dispersing species such as sardines (Roberts et al. 2010) and dolphins (Mendez et al. 2011), dispersal has been reported to be in the opposite direction, with the Agulhas Current forming the western boundary of the Indian Ocean.

In sharks, sexes often differ in their degree of dispersal and, hence, in their contribution to spatial genetic structure both within and among populations (Pereyra et al. 2010, Karl et al. 2011, Daly-Engel et al. 2012). Asymmetric migration rates among sexes, but also spatio-temporal variation in sex ratio, will then facilitate differential genetic signals between nuclear and mitochondrial markers. In most other coastal and pelagic shark species studied thus far, contrasting maternally and bi-parentally inherited genetic markers indicated dispersive males and philopatric females (Portnoy et al. 2010, Daly-Engel et al. 2012, Ashe et al. 2015). Data of the present study may suggest that male philopatry could account for the increased genetic differentiation found with the nuclear loci. Interestingly, tagging studies of the related species rig (*M. lentilacus*) found that females had a higher dispersal rate than males (Francis 1988). Further research by Boomer (2013) did not find clear evidence of genetic heterogeneity in either rig or Australian gummy shark but reported evidence of male-biased dispersal in Australian gummy shark, even though patterns were not strongly supported by the analyses applied. Future tagging studies using acoustic tracking, for example, could add to a better understanding of the regional movement patterns of *M. mustelus* as inferred here from genetic data.

Demographic history

In the present study, when using microsatellite data, the Wilcoxon signed-rank test for population bottlenecks detected a significant heterozygosity deficiency in almost all the study populations, indicating the likely effects of a recent demographic expansion event. However, significant heterozygosity deficiency may also arise from various other demographic factors, such as isolation by distance (Leblois et al. 2006), asymmetric gene flow (Paz-Vinas et al. 2013), or by immigration (Luikart & Cornuet 1998, Piry et al. 1999). In addition, heterozygosity deficiency can also arise in the earliest stages of a bottleneck, when a transient excess of alleles may exist, especially for markers evolving under a SMM mutational model (Cornuet & Luikart 1996).

When using mitochondrial DNA data, studies reconstructing the demographic history of various shark species, characterised by different life-history traits and habitat preferences, proposed that changes in climate during the Pleistocene epoch (ca. 2.6 million to 11700 yr before present, YBP) had a major impact on shaping the demographic history of sharks (O'Brien et al. 2013). Most notably, following the end of the last glacial maximum (LGM, ca. 20000 YBP), population expansion events have been reported for the whale shark *Rhincodon typus* (Vignaud et al. 2014) and *Mustelus* species (Pereyra et al. 2010, Boomer et al. 2012), whereas for the scalloped hammerhead shark *Sphyrna lewini* a population contraction (i.e. bottleneck) was reported (Nance et al. 2011). The absence of a well-calibrated molecular clock for *M. mustelus* presents a challenge for dating potential population expansion events and determining the effective population sizes associated with the ancestral and actual Θ-values. For *Mustelus* species, Boomer et al. (2012) (*M. antarcticus* and *M. lenticulatus*) and Pereyra et al. (2010) (*M. schmitti*) used averaged mutation rates from the scalloped hammerhead shark and lemon shark and from the bonnethead sharks, respectively. The latter species are very distant relatives of smoothhound sharks, and authors of the original studies claimed to be uncertain as to the reliability of these rate estimates (Duncan et al. 2006, Keeney & Heist 2006, Murray et al. 2008). For the reasons outlined above, no mutation rate was selected and applied in the present study.

Nevertheless, the findings of the present study strongly suggest a recent population expansion event [small $\tau = 2\mu T$ (mutational timescale) value of 0.5 and the large Θ-ratio ($\Theta_1/\Theta_0 = 17$)] that potentially coincides with the early Holocene (ca. 7000–11000 YBP) sea-level rise and warming (Carr et al. 2010, Dudgeon et al. 2012) that increased suitable coastal habitats for *M. mustelus* in southern Africa. An expansion following the LGM in *M. mustelus* is highly probable, considering that warming post-LGM caused population expansions in many marine and terrestrial organisms (Carr et al. 2010, Teske et al. 2011). In the future, estimates of a locus-specific mutation rate for the *ND4* gene in *M. mustelus* could assist in supporting the proposed timing of population expansion. Overall, this study detected no signal of a recent population bottleneck, which is not entirely unexpected since recent bottlenecks are transient and could go undetected by demographic history inferences due to variability in sampling and sampling period (Luikart & Cornuet 1998, Heller et al. 2013, Vignaud et al. 2014).

Implications for fisheries management of *M. mustelus*

In scope and scale, this work is one of the first regional population genetic studies for any elasmobranch species occurring in southern Africa. Overall, genetic analyses provide evidence that at least 2 differentiated populations exist for *M. mustelus*, one in the South-East Atlantic Ocean and one in the South-West Indian Ocean. Granted, much remains to be investigated about the life history of this species, but, given the genetic structure, small effective population size estimates and asymmetrical migration rates detected in this study, it is vital that stricter regulations be put in place for regional *M. mustelus*. In terms of fisheries management, a precautionary strategy should be taken where these populations are monitored as individual stocks (management units) rather than as a single panmictic population.

Acknowledgements. We thank the following persons and institutions for aiding in the acquisition of biological tissue samples (in alphabetical order): Adina Bosch, Michelle Soekoe, Oceans Research, South African Department of Agriculture, Forestry and Fisheries (DAFF; Melissa Goosen), South African Shark Conservancy and White Shark Africa. This study was funded by the National Research Foundation of South Africa.

LITERATURE CITED

Antao T, Lopes A, Lopes RJ, Beja-Pereira A, Luikart G (2008) LOSITAN: a workbench to detect molecular adaptation based on a F_{ST}-outlier method. BMC Bioinformatics 9:323

Ashe JL, Feldheim KA, Fields AT, Reyier EA and others (2015) Local population structure and context-dependent isolation by distance in a large coastal shark. Mar Ecol Prog Ser 520:203–216

Attwood CG, Peterson SL, Kerwath SE (2011) Bycatch in South Africa's inshore trawl fishery as determined from observer records. ICES J Mar Sci 68:2163–2174

Bandelt HJ, Forster P, Röhl A (1999) Median-joining networks for inferring intraspecific phylogenies. Mol Biol Evol 16:37–48

Beerli P (2006) Comparison of Bayesian and maximum-likelihood inference of population genetic parameters. Bioinformatics 22:341–345

Beerli P, Palczewski M (2010) Unified framework to evaluate panmixia and migration direction among multiple sampling locations. Genetics 185:313–326

Benavides MT, Feldheim KA, Duffy CA, Wintner S and others (2011) Phylogeography of the copper shark (*Carcharhinus brachyurus*) in the southern hemisphere: implications for the conservation of a coastal apex predator. Mar Freshw Res 62:861–869

Boomer JJ (2013) Molecular ecology and conservation of *Mustelus* (Gummy Shark, Rig) in Australasia. PhD dissertation, Macquarie University, Sydney

Boomer JJ, Peddemors V, Stow AJ (2010) Genetic data show that *Carcharhinus tilstoni* is not confined to the tropics, highlighting the importance of a multifaceted approach to species identification. J Fish Biol 77:1165–1172

Boomer JJ, Harcourt RG, Francis MP, Stow AJ (2012) Genetic divergence, speciation and biogeography of *Mustelus* (sharks) in the central Indo-Pacific and Australasia. Mol Phylogenet Evol 64:697–703

Briggs JC, Bowen BW (2012) A realignment of marine biogeographic provinces with particular reference to fish distributions. J Biogeogr 39:12–30

Carr AS, Bateman MD, Roberts DL, Murray-Wallace CV, Jacobs Z, Holmes PJ (2010) The last interglacial sea-level high stand on the southern Cape coastline of South Africa. Quat Res 73:351–363

Chabot CL (2015) Microsatellite loci confirm a lack of population connectivity among globally distributed populations of the tope shark *Galeorhinus galeus* (Triakidae). J Fish Biol 87:371–385

Chabot CL, Allen LG (2009) Global population structure of the tope (*Galeorhinus galeus*) inferred by mitochondrial control region sequence data. Mol Ecol 18: 545–552

Chabot CL, Espinoza M, Mascareñas Osorio I, Rocha Olivares A (2015) The effect of biogeographic and phylogeographic barriers on gene flow in the brown smoothhound shark, *Mustelus henlei*, in the northeastern Pacific. Ecol Evol 5:1585–1600

Cornuet JM, Luikart G (1996) Description and power analysis of two tests for detecting recent population bottlenecks from allele frequency data. Genetics 144:2001–2014

da Silva C (2007) The smoothhound shark (*M. mustelus*) fishery: status and prognosis. MSc thesis, Rhodes University, Rhodes

da Silva C, Bürgener M (2007) South Africa's demersal shark meat harvest. Traffic Bulletin 21:55–65

da Silva C, Kerwath SE, Attwood CG, Thorstad EB and others (2013) Quantifying the degree of protection afforded by a no-take marine reserve on an exploited shark. Afr J Mar Sci 35:57–66

Daly-Engel TS, Seraphin KD, Holland KN, Coffey JP, Nance HA, Toonen RT, Bowen BW (2012) Global phylogeography with mixed marker analysis reveals male-mediated dispersal in the endangered scalloped hammerhead shark (*Sphyrna lewini*). PLoS ONE 7:e29986

Darriba D, Taboada GL, Doallo R, Posada D (2012) jModelTest 2: more models, new heuristics and parallel computing. Nat Methods 9:772

Dudgeon CL, Blower DC, Broderick D, Giles JL and others (2012) A review of the application of molecular genetics for fisheries management and conservation of sharks and rays. J Fish Biol 8:1789–1843

Duncan KM, Martin AP, Bowen BW, de Couet GH (2006) Global phylogeography of the scalloped hammerhead shark (*Sphyrna lewini*). Mol Ecol 15:2239–2251

Earl DA, vonHoldt BM (2012) STRUCTURE HARVESTER: a website and program for visualizing STRUCTURE output and implementing the Evanno method. Conserv Genet Resour 4:359–361

Evanno G, Regnaut S, Goudet J (2005) Detecting the number of clusters of individuals using the software STRUCTURE: a simulation study. Mol Ecol 14:2611–2620

Excoffier L, Lischer HEL (2010) Arlequin suite version 3.5: a new series of programs to perform population genetics

analyses under Linux and Windows. Mol Ecol Resour 10: 564–567

Farrell ED, Clarke MW, Mariani S (2009) A simple genetic identification method for northeast Atlantic smoothhound sharks (*Mustelus* spp.). ICES J Mar Sci 66: 561–565

Francis MP (1988) Movement patterns of rig (*Mustelus lenticulatus*) tagged in southern New Zealand. N Z J Mar Freshw Res 22:259–272

Fu YX (1997) Statistical tests of neutrality of mutations against population growth, hitchhiking and background selection. Genetics 147:915–925

Fu YX, Li WH (1993) Statistical tests of neutrality of mutations. Genetics 133:693–709

Funk WC, McKay JK, Hohenlohe PA, Allendorf FW (2012) Harnessing genomics for delineating conservation units. Trends Ecol Evol 27:489–496

Harpending HC (1994) Signature of ancient population growth in a low-resolution mitochondrial DNA mismatch distribution. Hum Biol 66:591–600

Heller R, Chikhi L, Siegismund HR (2013) The confounding effect of population structure on Bayesian skyline plot inferences of demographic history. PLoS ONE 8:e62992

Henriques R, Potts WM, Sauer WHH, Shaw PW (2012) Evidence of deep genetic divergence between populations of an important recreational fishery species, *Lichia amia* L. 1758, around southern Africa. Afr J Mar Sci 34: 585–591

Henriques R, Potts WM, Sauer WHH, Santos CV, Shaw PW (2014) Population connectivity and phylogeography of a coastal fish, *Atractoscion aequidens* (Sciaenidae), across the Benguela Current region: evidence of an ancient vicariant event. PLoS ONE 9:e87907

Henriques R, Potts WM, Sauer WHH, Santos CV, Shaw PW (2015) Incipient genetic isolation of a temperate migratory coastal sciaenid fish (*Argyrosomus inodorus*) within the Benguela Cold Current system. Mar Biol Res 11: 423–429

Hutchings L, van der Lingen CD, Shannon LJ, Crawford RJM and others (2009) The Benguela Current: an ecosystem of four components. Prog Oceanogr 83:15–32

Jakobsson M, Rosenberg NA (2007) CLUMPP: a cluster matching and permutation program for dealing with label switching and multimodality in analysis of population structure. Bioinformatics 23:1801–1806

Jost L (2008) G_{ST} and its relatives do not measure differentiation. Mol Ecol 17:4015–4026

Kalinowski ST (2005) HP RARE 1.0: a computer program for performing rarefaction on measures of allelic richness. Mol Ecol Notes 5:187–189

Karl SA, Castro ALF, Lopez JA, Charvet P, Burgess GH (2011) Phylogeography and conservation of the bull shark (*Carcharhinus leucas*) inferred from mitochondrial and microsatellite DNA. Conserv Genet 12:371–382

Keeney DB, Heist EJ (2006) Worldwide phylogeography of the blacktip shark (*Carcharhinus limbatus*) inferred from mitochondrial DNA reveals isolation of western Atlantic populations coupled with recent Pacific dispersal. Mol Ecol 15:3669–3679

Leblois R, Estoup A, Streiff R (2006) Genetics of recent habitat contraction and reduction in population size: Does isolation by distance matter? Mol Ecol 15:3601–3615

Librado P, Rozas J (2009) DnaSP version 5: a software for comprehensive analysis of DNA polymorphism data. Bioinformatics 25:1451–1452

Luikart G, Cornuet JM (1998) Empirical evaluation of a test for identifying recently bottlenecked populations from allele frequency data. Conserv Biol 12:228–237

Maduna SN, Rossouw C, Roodt-Wilding R, Bester-van der Merwe AE (2014) Microsatellite cross-species amplification and utility in southern African elasmobranchs: a valuable resource for fisheries management and conservation. BMC Res Notes 7:352–364

Mendez M, Subramaniam A, Collins T, Minton G and others (2011) Molecular ecology meets remote sensing: environmental drivers to population structure of humpback dolphins in the western Indian Ocean. Heredity 107: 349–361

Miller MA, Pfeiffer W, Schwartz T (2010) Creating the CIPRES Science Gateway for inference of large phylogenetic trees. In: Proceedings of the Gateway computation and environment workshop (GCE). 14 Nov 2010, New Orleans, p 1–8

Moritz C (1994) Defining 'evolutionarily significant units' for conservation. Trends Ecol Evol 9:373–375

Murray BW, Wang JY, Yang SC, Stevens JD, Fisk A, Svavarsson J (2008) Mitochondrial cytochrome *b* variation in sleeper sharks (Squaliformes: Somniosidae). Mar Biol 153:1015–1022

Musick JA, Burgess GH, Camhi M, Cailliet G, Fordham S (2000) Management of sharks and their relatives (Elasmobranchii). Fisheries (Bethesda, Md) 25:9–13

Myers RA, Worm B (2003) Rapid worldwide depletion of predatory fish communities. Nature 423:280–283

Nance HA, Klimley P, Galvan-Magana F, Martinez-Ortiz J, Marko PB (2011) Demographic processes underlying subtle patterns of population structure in the scalloped hammerhead shark, *Sphyrna lewini*. PLoS ONE 6: e21459

O'Brien SM, Gallucci VF, Hauser L (2013) Effects of species biology on the historical demography of sharks and their implications for likely consequences of contemporary climate change. Conserv Genet 14:125–144

Ovenden JR (2013) Crinkles in connectivity: combining genetics and other types of data to estimate movement and interbreeding between populations. Mar Freshw Res 64:201–207

Ovenden JR, Berry O, Welch DJ, Buckworth RC, Dichmont CM (2013) Ocean's eleven: a critical evaluation of the role of population, evolutionary and molecular genetics in the management of wild fisheries. Fish Fish 15:1–35

Park S (2001) The Excel microsatellite toolkit. http://animalgenomics.ucd.ie/sdepark/ms-toolkit (downloaded on 27 February 2012)

Paz Vinas I, Quéméré E, Chikhi L, Loot G, Blanchet S (2013) The demographic history of populations experiencing asymmetric gene flow: combining simulated and empirical data. Mol Ecol 22:3279–3291

Peakall R, Smouse PE (2012) GenAlEx 6.5: genetic analysis in Excel: population genetic software for teaching and research—an update. Bioinformatics 28:2537–2539

Peeters FJC, Acheson R, Brummer GJA, de Ruijter WPM and others (2004) Vigorous exchange between the Indian and Atlantic Oceans at the end of the past five glacial periods. Nature 430:661–665

Pereyra S, Garcia G, Miller P, Oviedo S, Domingo A (2010) Low genetic diversity and population structure of the narrownose shark (*Mustelus schmitti*). Fish Res 106: 468–473

Piry S, Luikart G, Cornuet JM (1999) BOTTLENECK: a com-

puter program for detecting recent reductions in the effective population size using allele frequency data. J Hered 90:502–503

Portnoy DS, McDowell JR, Heist EJ, Musick JA, Graves JE (2010) World phylogeography and male-mediated gene flow in the sandbar shark, *Carcharhinus plumbeus*. Mol Ecol 19:1994–2010

Pritchard JK, Stephens M, Donnelly P (2000) Inference of population structure using multilocus genotype data. Genetics 155:945–959

R Development Core Team (2013) R: a language and environment for statistical computing. R Foundation for Statistical Computing, Vienna

Roberts MJ, van der Lingen CD, Whittle C, Van den Berg M (2010) Shelf currents, lee-trapped and transient eddies on the inshore boundary of the Agulhas Current, South Africa: their relevance to the KwaZulu-Natal sardine run. Afr J Mar Sci 32:423–447

Rosenberg NA (2004) DISTRUCT: a program for the graphical display of population structure. Mol Ecol Notes 4: 137–138

Rousset F (2008) GENEPOP'007: a complete re-implementation of the genepop software for Windows and Linux. Mol Ecol Resour 8:103–106

Saghai-Maroof MA, Solima KM, Jorgenson RA, Allard RW (1984) Ribosomal DNA spacerlength polymorphisms in barley: Mendelian inheritance, chromosomal location, and population dynamics. Proc Natl Acad Sci USA 81: 8014–8018

Saïdi B, Bradaï MN, Bouaïn A (2008) Reproductive biology of the smoothhound shark *Mustelus mustelus* (L.) in the Gulf of Gabès (south central Mediterranean Sea). J Fish Biol 72:1343–1354

Schneider S, Excoffier L (1999) Estimation of demographic parameters from the distribution of pairwise differences when the mutation rates vary among sites: application to human mitochondrial DNA. Genetics 152:1079–1089

Serena F, Mancusi C, Clò S, Ellis J, Valenti SV (2009) *Mustelus mustelus*. In: IUCN Red List of Threatened Species. www.iucnredlist.org (accessed 7 June 2014)

Smale MJ, Compagno LJV (1997) Life history and diet of two southern African smooth-hound sharks, *Mustelus mustelus* (Linnaeus, 1758) and *Mustelus palumbes* Smith, 1957 (Pisces: Triakidae). S Afr J Mar Sci 18: 229–248

Stevens JD, Bonfil R, Dulvy NK, Walker PA (2000) The effects of fishing on sharks, rays, and chimaeras (chondrichthyans), and the implications for marine ecosystems. ICES J Mar Sci 57:476–494

Tajima F (1989) Statistical method for testing the neutral mutation hypothesis by DNA polymorphism. Genetics 123:585–595

Tamura K, Peterson D, Peterson N, Stecher G, Nei M, Kumar S (2011) MEGA5: molecular evolutionary genetics analysis using maximum likelihood, evolutionary distance, and maximum parsimony methods. Mol Biol Evol 28: 2731–2739

Teske PR, von der Heyden S, McQuaid CD, Barker NP (2011) A review of marine phylogeography in southern Africa. S Afr J Sci 107:43–53

Van Oosterhout C, Hutchinson WF, Wills DPM, Shipley P (2004) MICROCHECKER: software for identifying and correcting genotyping errors in microsatellite data. Mol Ecol Notes 4:535–538

Vignaud TM, Maynard JA, Leblois R, Meekan MG and others (2014) Genetic structure of populations of whale sharks among ocean basins and evidence for their historic rise and recent decline. Mol Ecol 23:2590–2601

Ward RD, Zemlak TS, Innes BH, Last PR, Hebert PDN (2005) DNA barcoding Australia's fish species. Philos Trans R Soc Lond B Biol Sci 360:1847–1857

Weir BS, Cockerham CC (1984) Estimating *F*-statistics for the analysis of population structure. Evolution 38: 1358–1370

Editorial responsibility: Philippe Borsa, Montpellier, France

Submitted: April 1, 2015; Accepted: December 23, 2015
Proofs received from author(s): January 26, 2016